

# Electron-electron scattering effect on spin relaxation in multi-valley nanostructures

M.M. GLAZOV<sup>1</sup> and E.L. IVCHENKO<sup>1</sup>

<sup>1</sup> Ioffe Physical-Technical Institute RAS, 194021 St.-Petersburg, Russia

PACS 72.25.Rb – Spin relaxation and scattering

PACS 71.70.Ej – Spin-orbit coupling

**Abstract.** - We develop a theory of effects of electron-electron collisions on the Dyakonov-Perel' spin relaxation in multi-valley quantum wells. It is shown that the electron-electron scattering rate which governs the spin relaxation is different from that in a single-valley system. The theory is applied to Si/SiGe (001)-grown quantum wells where two valleys are simultaneously populated by free carriers. The dependences of the spin relaxation rate on temperature, electron concentration and valley-orbit splitting are calculated and discussed. We demonstrate that in a wide range of temperatures the electron-electron collisions can govern spin relaxation in high-quality Si/SiGe quantum wells.

**Introduction.** – Electron spin dynamics is among the most rapidly developing branches of the modern solid state physics due to the rise of spintronics [1, 2]. The prospects of spintronics which aims at the utilization of electron spin on equal grounds with its charge in novel semiconductor devices are related with the possibilities to create, control and manipulate the electron spins. The understanding of microscopic mechanisms of electron spin decoherence and relaxation is, hence, of high importance.

The main mechanism of electron spin relaxation in bulk semiconductors and semiconductor quantum wells (QWs) is Dyakonov-Perel' (or precession) mechanism [3, 4]. It is connected with the spin-orbit splitting of the conduction band states which acts as a wavevector ( $\mathbf{k}$ ) dependent effective magnetic field with the Larmor precession frequency  $\Omega_{\mathbf{k}}$ . Such an effective field arises only in non-centrosymmetric systems, the most widespread examples of them being bulk III-V semiconductors and QWs on their base. Although bulk Si and Ge crystals possess an inversion center, it has been demonstrated experimentally [5, 6] that the one-side modulation-doped Si/SiGe QW structures exhibit the Rashba effect and, in these structures, the electron spin relaxation is governed by precession mechanism as well. Recently, a theoretical estimation for the electron spin-orbit splitting in Si/SiGe heterostructures have been obtained by using the empirical tight-binding model computation [7, 8].

The electron spin precession in the effective magnetic

field is interrupted by the scattering events which change randomly the electron wavevector and, hence, the direction of the spin precession axis. Thus, the spin relaxation rate  $\tau_s^{-1}$  can be estimated as  $\langle \Omega_{\mathbf{k}}^2 \tau \rangle$  where angular brackets denote the averaging over the electron ensemble and  $\tau$  is the microscopic scattering time. Hence, the spin relaxation is slowed down by the scattering. It is evident that any momentum scattering process such as interaction of an electron with static impurities, interface imperfections or phonons stabilizes the spin. It is much less obvious that the electron-electron scattering can also suppress the Dyakonov-Perel' spin relaxation contributing additively to  $\tau^{-1}$  [9–13] and making the time  $\tau$  different from the momentum relaxation time. Indeed, it does not matter whether the electron wavevector is changed in the process of momentum scattering, due to the cyclotron motion or as a result of collision with other electrons [9]. It is established that nothing but an inclusion of the electron-electron scattering allows one to describe the temperature dependence of spin relaxation rates in high-quality GaAs QWs [12].

Here we address the electron-electron scattering effects on spin relaxation in Si/SiGe quantum wells. Their specific feature is the presence of several valleys [two in case of (001)-grown QWs] populated by electrons. The Coulomb scattering cannot transfer an electron from one valley into another although electrons from different valleys can interact with each other. We show here that the micro-

scopic scattering time  $\tau$  determined by electron-electron collisions in the multi-valley band system is different as compared with the single-valley case studied previously. The difference is related not only to the non-equal Fermi energies in the single-valley and multi-valley systems with equal electron densities but also to the different screening of Coulomb interaction in single- and multi-valley bands.

**Model.** – To be specific we consider Si/SiGe QWs grown along the axis  $z \parallel [001]$ . The conduction band states are formed from electron states in two  $\Delta$  valleys with the extrema  $\pm\mathbf{K}_0 = (0, 0, \pm K_0)$ , where  $K_0 \approx 0.8 \times 2\pi/a_0$  and  $a_0$  is the lattice constant. The electron reflection from the QW interfaces is accompanied by the intervalley transfers  $-\mathbf{K}_0 \rightarrow \mathbf{K}_0$  and vice versa which results in the valley-orbit splitting and formation of two subbands  $j = \pm$ , the lower subband  $j = -$  and the higher one  $j = +$ . The valley-orbit splitting  $\Delta_{\text{vo}}$ , depends on the QW width and interface properties. It may reach several meV in relatively thin quantum wells [7, 14]. The electron eigenstates  $|\mathbf{k}, j\rangle$  are superpositions of single-valley states and, in the envelope-function approach, can be written as

$$\Psi_j(\mathbf{r}) = e^{i(k_x x + k_y y)} \hat{C}_s \varphi(z) [c_{\mathbf{K}_0}^{(j)} \psi_{\mathbf{K}_0} + c_{-\mathbf{K}_0}^{(j)} \psi_{-\mathbf{K}_0}]. \quad (1)$$

Here  $\psi_{\pm\mathbf{K}_0}$  are the scalar bulk Bloch functions at the two extremum points  $\pm\mathbf{K}_0$ ,  $k_x, k_y$  are components of the two-dimensional wave vector  $\mathbf{k} \perp z$ ,  $\varphi(z)$  is the single-valley envelope function calculated neglecting the intervalley mixing and the spin-orbit interaction,  $c_{\pm\mathbf{K}_0}^{(j)}$  are coordinate independent scalar coefficients,  $|c_{\mathbf{K}_0}^{(j)}|^2 + |c_{-\mathbf{K}_0}^{(j)}|^2 = 1$ , and  $\hat{C}_s$  is a constant spinor describing the electron spin state. In QWs with asymmetric heteropotential (or with odd number of Si monoatomic planes) each of the subbands is split with respect to electron spin. The typical values of the spin-splitting have  $\mu\text{eV}$  range, i.e., they are much smaller than the valley-orbit splitting. Consequently, the electron Hamiltonian is decomposed into two partial spin-dependent Hamiltonians

$$\mathcal{H}^{(j)} = \frac{\hbar^2 k^2}{2m^*} \pm \frac{\Delta_{\text{vo}}}{2} + \frac{1}{2} \hbar \Omega_{\mathbf{k}}^{(j)} \cdot \boldsymbol{\sigma}, \quad (2)$$

describing electrons in each of the valley-orbit-split subbands. Here  $\boldsymbol{\sigma}$  is the vector composed of Pauli matrices and  $\Omega_{\mathbf{k}}$  is the angular frequency describing the spin splitting. The comparison of theoretical estimations and experimental data [8, 15, 16] shows that in the state-of-the-art samples the spin splitting is isotropic in the QW plane and has a symmetry of the Rashba type,  $\Omega_{\mathbf{k}}^{(j)} = \beta_j(k_y, -k_x, 0)$  and  $\Omega_{\mathbf{k}}^{(j)} \equiv |\Omega_{\mathbf{k}}^{(j)}| = |\beta_j|k$ . The arrangement of electron states is schematically shown in Fig. 1.

The kinetic theory of spin relaxation in Si/SiGe QWs is developed within the density matrix method. It is assumed that the valley-orbit splitting  $\Delta_{\text{vo}}$  can be comparable with characteristic energy of electrons and exceeds by far the inverse scattering time. In this case elements

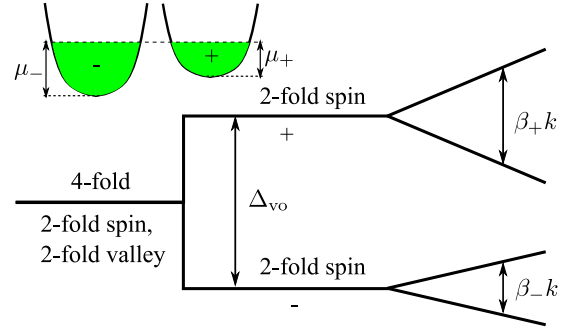


Fig. 1: Schematic subband structure in an  $n$ -doped Si/SiGe QW. The valley-orbit splitting,  $\Delta_{\text{vo}}$ , and spin splitting,  $\beta_+k$  and  $\beta_-k$ , are shown not to scale. Inset illustrates population of the subbands  $j = \pm$  by electrons,  $\mu_+$  and  $\mu_-$  are the chemical potentials referred to the subband bottoms.

of the density matrix nondiagonal in the subband indices  $j \neq j'$  can be disregarded whereas no restrictions are imposed on the density matrix in the spin subspace. Within each subband the spin-density matrix can be recast as

$$\rho_{\mathbf{k}}^{(j)} = f_{\mathbf{k}}^{(j)} + \mathbf{s}_{\mathbf{k}}^{(j)} \cdot \boldsymbol{\sigma} \quad (j = \pm), \quad (3)$$

where  $f_{\mathbf{k}}^{(j)}$  is the average occupation of the  $\mathbf{k}$  state in the subband  $j$ ,  $\mathbf{s}_{\mathbf{k}}^{(j)}$  is the average spin in this state, the symbol of the unity  $2 \times 2$  matrix is omitted.

The kinetic equation for the spin density matrix can be represented as a set of equations for the scalar  $f_{\mathbf{k}}^{(j)}$  and pseudovector  $\mathbf{s}_{\mathbf{k}}^{(j)}$  as follows

$$\frac{\partial f_{\mathbf{k}}^{(j)}}{\partial t} + Q_{\mathbf{k}}^{(j)} \{f, \mathbf{s}\} + \tilde{Q}^{(j)} \{f, \mathbf{s}\} = 0, \quad (4)$$

$$\frac{\partial \mathbf{s}_{\mathbf{k}}^{(j)}}{\partial t} + Q_{\mathbf{k}}^{(j)} \{\mathbf{s}, f\} + \tilde{Q}^{(j)} \{\mathbf{s}, f\} + \mathbf{s}_{\mathbf{k}}^{(j)} \times (\Omega_{\mathbf{k}}^{(j)} + \Omega_{C, \mathbf{k}}^{(j)}) = 0. \quad (5)$$

Here  $\Omega_{C, \mathbf{k}}^{(j)}$  is the effective field arising from the Hartree-Fock interaction in the spin-polarized electron gas [10, 17]. The scalar and vector electron-electron collision integrals, intra-valley ( $Q_{\mathbf{k}}^{(j)} \{f, \mathbf{s}\}, Q_{\mathbf{k}}^{(j)} \{\mathbf{s}, f\}$ ) and inter-valley ( $\tilde{Q}^{(j)} \{f, \mathbf{s}\}, \tilde{Q}^{(j)} \{\mathbf{s}, f\}$ ), are described in the next section.

**Intra- and inter-valley interaction.** – The collision integrals in Eqs. (4) and (5) describe the electron-electron scattering processes

$$(j_1 \mathbf{k} s_1) + (j_1' \mathbf{k}' s_1') \rightarrow (j_2 \mathbf{p} s_2) + (j_2' \mathbf{p}' s_2'), \quad (6)$$

where  $s_1, s_1'$  etc. are the electron spin components  $\pm 1/2$ . Because of a long-range character of the Coulomb interaction  $V_C$ , the intervalley scattering accompanied by transfer of the wavevector  $\sim 2K_0$  is strongly suppressed, and one can exclude from consideration any contributions due to the matrix elements  $\langle k'_x, k'_y, -K_0 | V_C | k_x, k_y, K_0 \rangle$  or  $\langle k'_x, k'_y, K_0 | V_C | k_x, k_y, -K_0 \rangle$ .

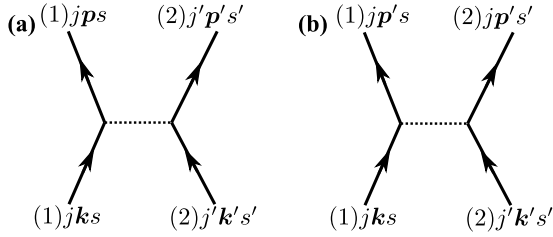


Fig. 2: Illustration of the direct (a) and exchange (b) Coulomb scattering between particle 1 with the spin  $s$  in the subband  $j$  and particle 2 with the spin  $s'$  and in the subband  $j'$ .

As a result, the effective matrix element describing the process (6) with allowance for the indistinguishability of the carriers reads (c.f. [10,18]):

$$\mathcal{M}(j_2 \mathbf{p} s_2; j'_2 \mathbf{p}' s'_2 | j_1 \mathbf{k} s_1; j'_1 \mathbf{k}' s'_1) = \delta_{\mathbf{k}+\mathbf{k}', \mathbf{p}+\mathbf{p}'} \times \quad (7)$$

$$(V_{\mathbf{k}-\mathbf{p}} \delta_{j_1 j_2} \delta_{j'_1 j'_2} \delta_{s_1 s_2} \delta_{s'_1 s'_2} - V_{\mathbf{k}-\mathbf{p}'} \delta_{j_1 j'_2} \delta_{j'_1 j_2} \delta_{s_1 s'_2} \delta_{s'_1 s_2}),$$

where  $V_{\mathbf{k}-\mathbf{p}}$  is the Fourier-transform component of the quasi-two-dimensional Coulomb potential. Figures 2(a) and 2(b) illustrate two contributions to the scattering process with a pair of electrons in the final state with the wave vectors  $\mathbf{p}$  and  $\mathbf{p}'$ . The first term in Eq. (7) is a Coulomb interaction where the first electron changes its wave vector from  $\mathbf{k}$  to  $\mathbf{p}$  while the second electron exhibits the scattering  $\mathbf{k}' \rightarrow \mathbf{p}'$ . The second term results from the scattering  $\mathbf{k} \rightarrow \mathbf{p}'$  and  $\mathbf{k}' \rightarrow \mathbf{p}$ , it enters Eq. (7) with the opposite sign. In the classical physics, the total effective cross-section is proportional to the sum  $|V_{\mathbf{k}-\mathbf{p}}|^2 + |V_{\mathbf{k}-\mathbf{p}'}|^2$  [19]. In quantum mechanics, for two electrons which have the same spin,  $s_1 = s_2$ , and occupy the same subband,  $j_1 = j_2$ , the cross-section has an additional interference term proportional to  $V_{\mathbf{k}-\mathbf{p}} V_{\mathbf{k}-\mathbf{p}'}$  [20]. Note, that a simple form of the above equation stems from neglecting the spin-orbit interaction in the processes of scattering [21].

The collision integrals in the kinetic equations are derived by using the standard diagram technique [10] and Eq. (7). Here we consider the experimentally typical situation of weak spin polarization,  $|\mathbf{s}_{\mathbf{k}}^{(j)}| \ll f_{\mathbf{k}}^{(j)}$  (although in GaAs the realization of a remarkable optical orientation of electron spins is also possible [17]). In this case the Hartree-Fock terms  $\Omega_{C,\mathbf{k}}^{(j)}$  in the kinetic equations (5) are unimportant and can be neglected. Let us present the collision integrals  $Q_{\mathbf{k}}^{(j)}\{f, \mathbf{s}\}$  and  $\tilde{Q}_{\mathbf{k}}^{(j)}\{f, \mathbf{s}\}$  in Eq. (4) in a convenient form

$$\frac{2\pi}{\hbar} \sum_{\mathbf{k}' \mathbf{p} \mathbf{p}'} \delta_{\mathbf{k}+\mathbf{k}', \mathbf{p}+\mathbf{p}'} \delta(E_{\mathbf{k}}^{(j)} + E_{\mathbf{k}'}^{(j)} - E_{\mathbf{p}}^{(j)} - E_{\mathbf{p}'}^{(j)}) P_{\mathbf{k} \mathbf{k}' \mathbf{p} \mathbf{p}'}^{(j)}$$

and

$$\frac{2\pi}{\hbar} \sum_{\mathbf{k}' \mathbf{p} \mathbf{p}'} \delta_{\mathbf{k}+\mathbf{k}', \mathbf{p}+\mathbf{p}'} \delta(E_{\mathbf{k}}^{(j)} + E_{\mathbf{k}'}^{(-j)} - E_{\mathbf{p}}^{(j)} - E_{\mathbf{p}'}^{(-j)}) \tilde{P}_{\mathbf{k} \mathbf{k}' \mathbf{p} \mathbf{p}'}^{(j)},$$

respectively. Here  $E_{\mathbf{k}}^{(j)}$  is the spin-independent part of the

electron energy equal to  $\hbar^2 k^2 / 2m^* \pm \Delta_{\text{vo}} / 2$ . The above-defined scalar functions take the form

$$P_{\mathbf{k} \mathbf{k}' \mathbf{p} \mathbf{p}'}^{(j)} = (2V_{\mathbf{k}-\mathbf{p}}^2 - V_{\mathbf{k}-\mathbf{p}'} V_{\mathbf{k}-\mathbf{p}}) \quad (8)$$

$$\times [f_{\mathbf{k}}^{(j)} f_{\mathbf{k}'}^{(j)} (1 - f_{\mathbf{p}}^{(j)} - f_{\mathbf{p}'}^{(j)}) - f_{\mathbf{p}}^{(j)} f_{\mathbf{p}'}^{(j)} (1 - f_{\mathbf{k}}^{(j)} - f_{\mathbf{k}'}^{(j)})],$$

for the intra-subband scattering, and

$$\tilde{P}_{\mathbf{k} \mathbf{k}' \mathbf{p} \mathbf{p}'}^{(j)} = 2V_{\mathbf{k}-\mathbf{p}}^2 \quad (9)$$

$$\times [f_{\mathbf{k}}^{(j)} f_{\mathbf{k}'}^{(-j)} (1 - f_{\mathbf{p}}^{(j)} - f_{\mathbf{p}'}^{(-j)}) - f_{\mathbf{p}}^{(j)} f_{\mathbf{p}'}^{(-j)} (1 - f_{\mathbf{k}}^{(j)} - f_{\mathbf{k}'}^{(-j)})],$$

for the subband-subband scattering, similarly to the case of electron-hole scattering and electron-electron scattering in a quantum well with several occupied size-quantized subbands [23]. It is worth mentioning that for the scattering between different particles (e.g. electrons and ions in plasma) the scattering rates are by the factor of 2 smaller as compared with those given by Eq. (9) because of the absence of the contribution given by Fig. 2(b).

For the pseudovector collision integrals  $\tilde{Q}_{\mathbf{k}}^{(j)}\{\mathbf{s}, f\}$  and  $\tilde{Q}_{\mathbf{k}}^{(j)}\{f, \mathbf{s}\}$ , we similarly introduce the pseudovectors  $\tilde{P}_{\mathbf{k} \mathbf{k}' \mathbf{p} \mathbf{p}'}^{(j)}$  and  $\tilde{P}_{\mathbf{k} \mathbf{k}' \mathbf{p} \mathbf{p}'}^{(j)}$  which are given, respectively, by

$$(2V_{\mathbf{k}-\mathbf{p}}^2 - V_{\mathbf{k}-\mathbf{p}} V_{\mathbf{k}-\mathbf{p}'})[\mathbf{s}_{\mathbf{k}}^{(j)} F_j(\mathbf{k}'; \mathbf{p}, \mathbf{p}') - \mathbf{s}_{\mathbf{p}'}^{(j)} F_j(\mathbf{p}'; \mathbf{k}, \mathbf{k}')] - V_{\mathbf{k}-\mathbf{p}} V_{\mathbf{k}-\mathbf{p}'} [\mathbf{s}_{\mathbf{k}'}^{(j)} F_j(\mathbf{k}; \mathbf{p}, \mathbf{p}') - \mathbf{s}_{\mathbf{p}}^{(j)} F_j(\mathbf{p}'; \mathbf{k}, \mathbf{k}')] , \quad (10)$$

$$2V_{\mathbf{k}-\mathbf{p}}^2 [\mathbf{s}_{\mathbf{k}}^{(j)} \tilde{F}_j(\mathbf{k}'; \mathbf{p}, \mathbf{p}') - \mathbf{s}_{\mathbf{p}'}^{(j)} \tilde{F}_j(\mathbf{p}'; \mathbf{k}, \mathbf{k}')] ,$$

where  $F_j(\mathbf{k}_1; \mathbf{k}_2, \mathbf{k}_3) = f_{\mathbf{k}_1}^{(j)} (1 - f_{\mathbf{k}_2}^{(j)} - f_{\mathbf{k}_3}^{(j)}) + f_{\mathbf{k}_2}^{(j)} f_{\mathbf{k}_3}^{(j)}$  and  $\tilde{F}_j(\mathbf{k}_1; \mathbf{k}_2, \mathbf{k}_3) = f_{\mathbf{k}_1}^{(-j)} (1 - f_{\mathbf{k}_2}^{(j)} - f_{\mathbf{k}_3}^{(-j)}) + f_{\mathbf{k}_2}^{(j)} f_{\mathbf{k}_3}^{(-j)}$ . Similar collision integrals for subband-subband scattering were derived in Ref. [24] for the electron-electron collisions in GaAs quantum well with  $\Gamma$  and  $L$  occupied valleys.

Before turning to the spin relaxation times we discuss the screening of Coulomb potential in a multivalley system. Assuming that the QW width is small enough to permit the electrons to be treated as strictly two-dimensional, the Fourier transform of Coulomb potential may be written approximately as, e.g., Refs. [23, 25],

$$V_{\mathbf{q}} = \frac{2\pi e^2}{S \varepsilon(q + q_s)}, \quad (11)$$

where  $e$  is the elementary charge,  $S$  is the normalization area,  $\varepsilon$  is the static dielectric constant, and  $q_s$  is the inverse screening length given by

$$q_s = \frac{2m^* e^2}{\varepsilon \hbar^2} \sum_j \left(1 + e^{-\mu_j / k_B T}\right)^{-1}. \quad (12)$$

Here the summation is carried out over occupied subbands,  $k_B$  is Boltzmann's constant,  $T$  is the absolute temperature,  $\mu_j$  is the chemical potential of electrons referred to the bottom of the  $j$ -th subband, see inset in Fig. 1. In the limit of non-degenerate electrons,  $\exp(-\mu_j / k_B T) \gg$

1, and the screening is negligible. If electrons are strongly degenerate,  $\exp(-\mu_j/k_B T) \ll 1$ , each occupied subband yields the same contribution  $2m^*e^2/(\epsilon\hbar^2)$  and the total inverse screening length increases proportionally to the number of occupied subbands.

**Spin relaxation times.** – Kinetic equations (4), (5) are solved following the standard procedure [10]. We consider the equilibrium electron distribution with  $f_{\mathbf{k}}^{(j)} = \{\exp[(E_{\mathbf{k}}^{(j)} - \mu_j)/k_B T] + 1\}^{-1}$  and seek the spin distribution function  $\mathbf{s}_{\mathbf{k}}^{(j)}$  in the form

$$\mathbf{s}_{\mathbf{k}}^{(j)} = \bar{\mathbf{s}}_{\mathbf{k}}^{(j)} + \delta\mathbf{s}_{\mathbf{k}}^{(j)}. \quad (13)$$

Here  $\bar{\mathbf{s}}_{\mathbf{k}}^{(j)}$  is a quasi-equilibrium axially-symmetric spin distribution function related to the initially created total electron spin in the  $j$ -th subband by  $\mathbf{S}^{(j)} = \sum_{\mathbf{k}} \bar{\mathbf{s}}_{\mathbf{k}}^{(j)}$ , and  $\delta\mathbf{s}_{\mathbf{k}}^{(j)}$  is a non-equilibrium correction resulting from the electron spin precession around the vector  $\Omega_{\mathbf{k}}^{(j)}$ . Below we assume  $\Omega_{\mathbf{k}}^{(j)}\tau \ll 1$  (the collision dominated regime) where  $\tau$  is the typical scattering time. This condition is surely satisfied in Si/SiGe QWs [5, 6, 15]. Since the collision integrals  $\mathbf{Q}_{\mathbf{k}}^{(j)}\{\delta\mathbf{s}, f\}$  and  $\tilde{\mathbf{Q}}_{\mathbf{k}}^{(j)}\{\delta\mathbf{s}, f\}$  conserve the angular dependence of  $\delta\mathbf{s}_{\mathbf{k}}^{(j)}$  one can present this correction as follows

$$\delta\mathbf{s}_{\mathbf{k}}^{(j)} = -F_{\mathbf{k}}^{(j)} \left( \bar{\mathbf{s}}_{\mathbf{k}}^{(j)} \times \Omega_{\mathbf{k}}^{(j)} \right),$$

where  $F_{\mathbf{k}}^{(j)}$  is a function of  $k = |\mathbf{k}|$ . It can be found from the solution of linearized Eq. (5). For the Rashba-like spin splitting we eventually arrive at

$$\frac{1}{\tau_{s,zz}^{(j)}} = \sum_{\mathbf{k}} \Omega_{\mathbf{k}}^{(j)2} F_{\mathbf{k}}^{(j)} = \beta_j^2 \sum_{\mathbf{k}} k^2 F_{\mathbf{k}}^{(j)}, \quad (14)$$

and  $\tau_{s,xx}^{(j)} = \tau_{s,yy}^{(j)} = 2\tau_{s,zz}^{(j)}$ , where  $\tau_{s,\alpha\alpha}^{(j)}$  is the spin relaxation time in the  $j$ -th subband for the spin oriented along the  $\alpha$  axis.

In the limits of degenerate and non-degenerate statistics it is instructive to introduce an effective scattering time  $\tau_j^*$  in the  $j$ th subband defined by

$$\frac{1}{\tau_{s,zz}^{(j)}} = \Omega_j^2 \tau_j^*, \quad (15)$$

where the characteristic spin precession frequency  $\Omega_j = \beta_j k_F^{(j)}$  for a degenerate electron gas and  $\Omega_j = \beta_j k_T$  for a non-degenerate gas,  $k_F^{(j)}$  is the Fermi wavevector at zero temperature in a given subband, and  $k_T$  is the thermal wavevector  $\sqrt{2m^*k_B T}/\hbar$ . In fact, the time  $\tau_j^*$  is a microscopic electron-electron scattering time governing the Dyakonov-Perel' spin relaxation in each subband. Comparing Eqs. (14) and (15) we obtain

$$\tau_j^* = \sum_{\mathbf{k}} \frac{k^2}{k_F^{(j)2}} F_{\mathbf{k}}^{(j)} \quad (\text{degenerate electrons}), \quad (16)$$

$$\tau_j^* = \sum_{\mathbf{k}} \frac{k^2}{k_T^2} F_{\mathbf{k}}^{(j)} \quad (\text{non-degenerate electrons}). \quad (17)$$

**Results and discussion.** – Below we present analytical and numerical results for the microscopic scattering times  $\tau_j^*$  which govern Dyakonov-Perel' spin relaxation in multivalley QWs. In order to emphasize the role of electron-electron interaction the effects of single-particle momentum scattering are ignored, they can be taken into account by inclusion into the right-hand side of kinetic equation (5) the collision term  $-\delta\mathbf{s}_{\mathbf{k}}/\tau_p$ , where  $\tau_p$  is the momentum scattering time.

For the *non-degenerate* electron gas, one can neglect the screening of the electron-electron interaction and the collision integrals describing intra-subband and subband-subband  $\mathbf{Q}_{\mathbf{k}}\{\mathbf{s}, f\}$  and  $\tilde{\mathbf{Q}}_{\mathbf{k}}\{\mathbf{s}, f\}$  differ, apart from the terms  $V_{\mathbf{k}-\mathbf{p}}V_{\mathbf{k}-\mathbf{p}'}$ , by a common factor,  $f_{\mathbf{k}'}^{(j)}/f_{\mathbf{k}'}^{(-j)}$ , resulting from different populations of the valley-orbit split subbands. The inverse microscopic scattering time  $\tau^{*-1}$  has two additive contributions caused by the collision of electrons within the same subband and electrons in different subbands each of those being proportional to the number of electrons in a given subband. Neglecting the terms  $V_{\mathbf{k}-\mathbf{p}}V_{\mathbf{k}-\mathbf{p}'}$  and making use of the results for a single valley [9, 10] we have

$$\tau_-^* = \tau_+^* = \tau_{ee}^{(B)}, \quad (18)$$

where  $\tau_{ee}^{(B)}$  is the electron-electron scattering time which governs spin relaxation in the single valley structure occupied by electrons with total concentration  $N = N_+ + N_-$ ,

$$\tau_{ee}^{(B)} = \frac{\hbar\epsilon^2 k_B T}{e^4 N} I, \quad (19)$$

and  $I$  is a numerical factor which, for strictly two-dimensional electrons, equals to  $\approx 0.027$  [9, 10]. The scattering times in the subbands are, therefore, the same, since it does not matter whether an electron scatters by an electron in the same or in the other subband. The spin relaxation times in the valley-orbit split subbands are different only due to the difference of the spin splittings in the subbands. Note, that the allowance for the interference contributions  $V_{\mathbf{k}-\mathbf{p}}V_{\mathbf{k}-\mathbf{p}'}$  results in a slight ( $\approx 4\%$ ) increase of the constant  $I$  for the intrasubband interaction [9, 10], hence, these terms can be safely neglected.

Now we turn to low temperatures where the electrons are *degenerate*. Figure 3 depicts the dependence of the scattering times  $\tau_{\pm}^*$  on  $\Delta_{\text{vo}}$  related to the Fermi energy  $E_F$  of electrons of the same concentration populating a single valley. In this case the electron-electron collisions are suppressed due to the Pauli principle and, moreover, the screening parameter  $q_s$  is not negligible. This gives rise to two additional competing factors which have effect on the difference between the scattering rates in single- and two-valley systems. First, the electrons are redistributed between valleys which results in a decrease of electron concentration in each valley and, consequently, in an enhancement of the scattering rate due to reducing the Pauli blocking. Second, the screening efficiency increases and, therefore, the scattering rates are decreased. Due to

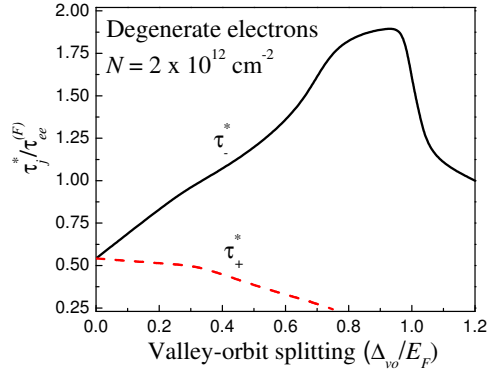


Fig. 3: Electron-electron scattering times  $\tau_{\pm}^*$  in a two-valley QW as a function of the valley-orbit splitting. The times are presented in units of the similar scattering time in a single valley with the same carrier density and temperature. Black solid line corresponds to the lower, more populated, valley while red dashed line describes the upper, less populated, valley. The calculation is carried out for the degenerate electron gas, temperature  $T = 8.2$  K,  $N = 2 \times 10^{12} \text{ cm}^{-2}$ ,  $E_F$  is the Fermi energy in the single valley with the same concentration  $N$ . Other parameters used in the calculation correspond to Si/SiGe QWs:  $\alpha = 12$ , and  $m^* = 0.191m_0$ , where  $m_0$  is the free electron mass.

the competition between these two factors the electron-electron scattering time can be both longer and shorter in a two-valley system as compared with a single valley.

A simple analytical expression for the electron-electron scattering time can be derived in the absence of intervalley mixing in which case  $N_+ = N_- = N/2$ ,  $\mu_+ = \mu_- = E_F/2$  and  $\tau_+^* = \tau_-^* \equiv \tau^*$ . Let us introduce the electron-electron scattering rate governing the spin relaxation in a single-valley system with the degenerate electrons of the total density  $N$  [10]

$$\frac{1}{\tau_{ee}^{(F)}} \approx 3.4 \frac{(k_B T)^2}{\hbar E_F} = 3.4 \frac{m(k_B T)^2}{\pi \hbar^3 N}. \quad (20)$$

In a two-valley system at,  $k_B T \ll \mu$ , one has

$$\tau^* = \frac{J}{4} \tau_{ee}^{(F)}. \quad (21)$$

The factor  $1/4$  in Eq. (21) results from allowance for the valley-valley interaction and takes also into account that the Fermi energy in each valley is twice smaller as compared with the single-valley system with the same total density. The factor  $J$  describes the modification due to allowance for the screening. In the limit of  $k_F = \sqrt{m^* E_F / \hbar^2} \ll q_s$ , i.e., where the screening is so strong that the electron-electron interaction is effectively short-range,  $J = 4$  since the inverse screening length is twice smaller as compared with single valley system and, hence, the scattering probability decreases by a factor of 4. In real QWs  $k_F$  and  $q_s$  can be comparable [26] and  $J$  ranges from 1 to 4 depending on the electron concentration. For

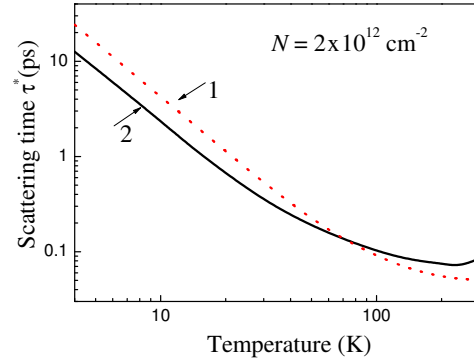


Fig. 4: Electron-electron scattering times as a function of temperature calculated from Eq. (16) for single valley (curve 1) and two-valley (curve 2) quantum wells. The valley-orbit splitting is set to zero. The electron concentration  $N = 2 \times 10^{12} \text{ cm}^{-2}$ . Other parameters are the same as in caption to Fig. 3.

the parameters used in the calculation of Fig. 3 the factor  $J \approx 2.2$  and, at  $\Delta_{vo} \ll E_F$ , the ratio  $\tau^*/\tau_{ee}^{(F)}$  is close to 0.55. In QW structures with a large number of unmixed valleys,  $n_v \gg 1$ , like (111)-grown Si MOSFET structures and degenerate electrons, the scattering time  $\tau^*$  increases  $\propto n_v$  due to the competing effects of enhancing screening and decreasing Pauli blocking. With the increasing valley-orbit splitting, the electron-electron scattering time in the lower valley,  $\tau_-$ , becomes longer and the scattering time  $\tau_+$  shortens. This is a result of electron redistribution downward to the lower subband and an enhancement of Pauli blocking there. In the upper subband the electron density decreases and the Pauli blocking becomes weaker. If all the electrons fill the lower subband the scattering time,  $\tau_-$ , rapidly drops because the screening parameter  $q_s$  reduces by a factor of 2 and approaches the single-valley value, Fig. 3. One can also see from this figure that the electron-electron scattering time  $\tau_-^*$  can be both shorter and longer than that for the single-valley system.

For non-zero valley-orbit splitting, the spin relaxation times of the electrons in the two subbands  $j = \pm$  can be different due to the following reasons: (i) difference of the electron-electron scattering times  $\tau_+^* \neq \tau_-^*$ , (ii) difference of the Fermi wavevectors  $k_F^{(j)}$  and (iii) difference of the spin-splitting constants  $\beta_+ \neq \beta_-$ . Weak intervalley scattering characterized by the time  $\tau_v \gg \tau_{\pm}^*, \tau_p$  may lead to the efficient intermixing of spins in different valleys. The observed spin relaxation time for the spin along one of the main axes  $\alpha$  is, hence,

$$T_{s,\alpha\alpha} = \frac{2\tau_{s,\alpha\alpha}^{(+)}\tau_{s,\alpha\alpha}^{(-)}}{\tau_{s,\alpha\alpha}^{(+)} + \tau_{s,\alpha\alpha}^{(-)}},$$

provided  $\tau_v \ll \tau_{s,\alpha\alpha}^{(\pm)}$ .

Finally, in Fig. 4 the calculated temperature dependence of the electron-electron scattering time is depicted. Dotted curve represents a single-valley system, solid curve shows the calculation for the two-valley QW with zero valley-

orbit splitting and the same concentration of carriers. We remind that according to Eq. (15) the spin relaxation rate is obtained as a product of  $\tau^*$  defined by Eq. (16) and the squared spin precession frequency taken at the Fermi level at zero temperature. The qualitative behavior of these two curves is similar: with the temperature increase the scattering time shortens as  $\tau^* \propto T^{-2}$  [see Eq. (21)] due to the weakening of Pauli blocking and reaches a minimum (seen in the figure only for the two-valley structure) caused by the transition to the non-degenerate case. This transition takes place at a smaller temperature for the two-valley system because the carrier concentration in each valley is twice smaller. For the accepted parameters the scattering time in the two-valley system, in comparison with the single-valley system, is shorter at lower temperatures and longer at higher temperatures.

One can see from Fig. 4 that the scattering time  $\tau^*$  has a picosecond scale in a wide range of temperatures. In the state-of-the-art Si/SiGe QWs where the spin relaxation was studied the momentum scattering time  $\tau_p$  was about 10 ps for even smaller carrier concentrations than those taken in our calculation. Therefore, electron-electron collisions play a substantial role in controlling the spin relaxation in those Si/SiGe structures.

**Conclusions.** – We have developed a theory of electron-electron scattering effect on the Dyakonov-Perel’ spin relaxation in multi-valley semiconductor QWs. We have shown that, although the intervalley scattering of electrons is suppressed, the interaction of electrons occupying different valley-orbit split subbands influences the spin relaxation. The electron-electron scattering rates in single and multi-valley systems are different due to (i) redistribution of electrons between the subbands, and (ii) an enhancement of screening in the two-valley systems.

The values of electron-electron scattering times in high-mobility Si/SiGe QWs with two occupied valleys may be comparable and even shorter than the momentum scattering time in a wide range of temperatures. Therefore, in these structures the electron spin relaxation can be controlled by electron-electron scattering.

\* \* \*

Authors thank Ming-Wei Wu, W. Jantsch and Z. Wilamowski for valuable discussions and M.O. Nestoklon for critical reading of the manuscript. We gratefully acknowledge the financial support from RFBR, Programs of RAS and “Dynasty” Foundation — ICFPM.

## REFERENCES

- [1] DYAKONOV M. I., (Editor) *Spin Physics in Semiconductors* 2008.
- [2] ZUTIC I., FABIAN J. and SARMA S. D., *Rev. Mod. Phys.* , **76** (2004) 323.
- [3] DYAKONOV M. I. and PEREL’ V. I., *Sov. Phys. Solid State* , **13** (1972) 3023.
- [4] DYAKONOV M. and KACHOROVSKII V., *Sov. Phys. Semicond.* , **20** (1986) 110.
- [5] WILAMOWSKI Z., JANTSCH W., MALISSA H. and RÖSSLER U., *Phys. Rev. B* , **66** (2002) 195315.
- [6] WILAMOWSKI Z. and JANTSCH W., *Phys. Rev. B* , **69** (2004) 035328.
- [7] NESTOKLON M. O., GOLUB L. E. and IVCHENKO E. L., *Phys. Rev. B* , **73** (2006) 235334.
- [8] NESTOKLON M. O., IVCHENKO E. L., JANCU J.-M. and VOISIN P., *Phys. Rev. B* , **77** (2008) 155328.
- [9] GLAZOV M. and IVCHENKO E., *JETP Letters* , **75** (2002) 403.
- [10] GLAZOV M. and IVCHENKO E., *JETP* , **99** (2004) 1279.
- [11] BRAND M. A., MALINOWSKI A., KARIMOV O. Z., MARDEN P. A., HARLEY R. T., SHIELDS A. J., SANVITTO D., RITCHIE D. A. and SIMMONS M. Y., *Phys. Rev. Lett.* , **89** (2002) 236601.
- [12] LEYLAND W. J. H., JOHN G. H., HARLEY R. T., GLAZOV M. M., IVCHENKO E. L., RITCHIE D. A., FARRER I., SHIELDS A. J. and HENINI M., *Phys. Rev. B* , **75** (2007) 165309.
- [13] WENG M. Q. and WU M. W., *Phys. Rev. B* , **68** (2003) 75312.
- [14] BOYKIN T. B., KLIMECK G., FRIESEN M., COPPERSMITH S. N., VON ALLMEN P., OYAFUSO F. and LEE S., *Phys. Rev. B* , **70** (2004) 165325.
- [15] GLAZOV M. M., *Phys. Rev. B* , **70** (2004) 195314.
- [16] WILAMOWSKI Z., MALISSA H., SCHÄFFLER F. and JANTSCH W., *Phys. Rev. Lett.*, **98** (2007) 187203.
- [17] STICH D., ZHOU J., KORN T., SCHULZ R., SCHUH D., WEGSCHEIDER W., WU M. W. and SCHÜLLER C., *Phys. Rev. B*, **76** (2007) 205301.
- [18] PUNNOOSE A. and FINKEL’STEIN A. M., *Science* , **310** (2005) 289.
- [19] LANDAU L. D. and LIFSHITZ E. M., *Mechanics* (Butterworth-Heinemann, Oxford) 1976.
- [20] LANDAU L. D. and LIFSHITZ E. M., *Quantum Mechanics (Non-Relativistic Theory)* (Butterworth-Heinemann, Oxford) 1977.
- [21] GLAZOV M. M. and KULAKOVSKII V. D., *Phys. Rev. B*, **79** (2009) 195305.
- [22] GLAZOV M. M. and IVCHENKO E. L., *Optical Properties of 2D Systems with Interacting Electrons*, eds. by W.J. Ossaou and R. Suris, *NATO Science Series*, Vol. 119 (2003) p. 181.
- [23] H. HAUG and A. P. JAUHO, *Quantum kinetics in transport and optics of semiconductors* (Springer, Berlin) 1996; DÜR M., GOODNICK S. M. and LUGLI P., *Phys. Rev. B* , **54** (1996) 17794.
- [24] ZHANG P., ZHOU J. and M. W. WU, *Phys. Rev. B*, **77** (2008) 235323.
- [25] ANDO T., FOWLER A. B. and STERN F., *Rev. Mod. Phys.* , **54** (1982) 437.
- [26] JUNGWIRTH T. and MACDONALD A. H., *Phys. Rev. B* , **53** (1996) 7403.